Peripheral Bone Status in Rheumatoid Arthritis Evaluated by Digital X-Ray Radiogrammetry and Compared with Multisite Quantitative Ultrasound

J. Böttcher,[1] A. Pfeil,[1] H. Mentzel,[1] A. Kramer,[1] M.-L. Schäfer,[1] G. Lehmann,[2] T. Eidner,[2] A. Petrovitch,[1] A. Malich,[1] G. Hein,[2] W. A. Kaiser[1]

[1]Institute of Diagnostic and Interventional Radiology, Friedrich-Schiller University Jena, Jena, Germany
[2]Department of Rheumatology and Osteology, Friedrich-Schiller University Jena, Jena, Germany

Abstract. The development of secondary osteoporosis in rheumatoid arthritis (RA) has recently become well recognized, characterized by demineralization at axial and in particular periarticular peripheral bone sites. Our aim was to evaluate multisite quantitative ultrasound (QUS) compared to digital X-ray radiogrammetry (DXR) by the quantification of cortical bone loss dependent on the severity of RA. Fifty-three patients with verified RA underwent QUS measurements (Sunlight Omnisense 7000) with estimation of the speed of sound (QUS-SOS) at the distal radius and at the phalanx of the third digit. Also, bone mineral density (DXR-BMD) and metacarpal index (DXR-MCI) were estimated on metacarpals II-IV using DXR technology. Additionally, Larsen score and Steinbroker stage were assessed. Disease activity of RA was estimated by disease activity score 28 (DAS 28). For the group with minor disease activity ($3.2 \leq DAS \leq 5.1$), QUS-SOS (phalanx) showed a significant association to DXR-BMD (R = 0.66) and DXR-MCI (R = 0.52). In the case of accentuated disease activity (DAS > 5.1), QUS-SOS of the radius revealed a significant correlation to DXR-BMD (R = 0.71) and DXR-MCI (R = 0.84), whereas for QUS-SOS (phalanx) no significant association to the DXR parameters was shown. The DXR parameters and, to a lesser extent, the QUS data also demonstrated pronounced declines in the case of accentuated disease activity (DAS > 5.1). Both DXR-BMD (-25.9%, $P < 0.01$) and DXR-MCI (-38.6%, $P < 0.01$) revealed a notable reduction dependent on the severity of RA. Otherwise, QUS-SOS marginally decreased, with -2.6% (radius) and -3.9% (phalanx). DXR revealed a significant reduction of DXR-BMD as well as DXR-MCI dependent on the severity of RA and surpassed multisite QUS as a promising diagnostic tool.

Key words: Digital X-ray radiogrammetry — Quantitative ultrasound — Rheumatoid arthritis — Bone mineral density — Speed of sound

Correspondence to: J. Böttcher; E-mail: joachim.boettcher@med.uni-jena.de

Rheumatoid arthritis (RA) is a systemic and chronic disease characterized by inflammation of the joints, frequently resulting in impairment of function and destruction of the affected small joints of the hand. The hand shows the earliest manifestations of RA, and the destruction of small joints correlates well with alterations seen on radiographs of large joints [1−3].

Osteoporosis in RA patients occurs in two forms: periarticular and generalized. Periarticular osteoporosis, a typical phenomenon in early RA, is seen in near proximity to the inflamed joints and is closely related to disease activity [4, 5]. Generalized osteoporosis, in contrast, affects the axial and appendicular bones and occurs during the course of RA caused by steroid therapy, generalized disease activity, and immobility [6−8].

RA-specific periarticular osteoporosis is known to occur before visible erosions are detectable, and this accelerated bone turnover can continue even in the absence of other signs of disease activity. The clinical evaluation of secondary osteoporosis in patients with RA is essential because RA tends to affect the small joints of the hands first and, preferentially, precise quantification of demineralization in the hand may predict joint destruction. Alenfeld et al. [9] and Devlin et al. [10] revealed a greater degree of bone loss in the subregions of phalanges and metacarpals compared to whole-hand bone mineral density (BMD) measured by dual-energy X-ray absorptiometry (DXA). In an extensive study, Njeh et al. [11] documented that bone loss estimated by quantitative ultrasound (QUS) at the proximal phalanges is significantly accentuated in patients with RA compared to patients receiving corticoid therapy, whereas the BMD of the lumbar spine measured by DXA was comparatively higher in patients with RA. Altogether these findings seem to point at the benefit of peripheral techniques for estimation of peripheral bone status and in particular for quantifica-

tion of RA-specific periarticular osteoporosis compared to axial measurement sites [12].

Digital X-ray radiogrammetry (DXR) is a new diagnostic tool for the measurement of cortical BMD (DXR-BMD) on metacarpals using digitized radiographs and based on conventional radiogrammetry [13]. Several studies have published normative values and data on reproducibility for DXR [14–21]. DXR seems to bridge the gap between conventional radiogrammetry and densitometry by estimating BMD from radiogeometric measurements [18, 20, 21].

Recent studies have also shown that DXR is able to detect disease progression in RA [22–24]. Several studies have compared DXR and DXA and shown a superior capability of DXR compared to DXA in detecting and quantifying bone loss in the hand of RA patients [22, 23].

Another innovative technique to evaluate bone characteristics is QUS [25]. The advantages of QUS include the fact that the equipment is inexpensive, small, and portable and does not involve the use of ionizing radiation [26]. Furthermore, QUS provides data on bone quality (i.e., elasticity and trabecular connectivity of bone tissue) and bone quantity (i.e., BMD). The ultrasonic technology involves the passing of sound waves through the bone matrix, which allows estimation of attenuation (broadband ultrasound attenuation, BUA) and speed of sound (SOS) through bone tissue [27]. SOS is related to the connectivity, elasticity, and stiffness of bone, whereas BUA is believed to be related to BMD and the trabecular microarchitecture [28–32]. Both cross-sectional and prospective studies have demonstrated that QUS can be used to distinguish normal from osteoporotic individuals nearly as effectively as established bone densitometric methods. Furthermore, QUS is partly independent of BMD, which points at the fact that QUS reveals data not only about BMD (i.e., bone quantity) but also about structural and mechanical bone properties [33–35].

Only a few studies have investigated alterations of bone tissue in RA quantified by QUS at single measurement sites with transmission [9, 11, 26, 36]. These data suggest that bone quality of calcaneus and fingers is clearly affected in patients suffering from RA using the DBM Sonic (Igea, Italy) technology [11, 26].

A recently available technology based on multisite QUS, the Omnisense 7000 device (Sunlight Medical, Tel Aviv, Israel), functions by accessing the bone from only one site, apparently showing no influence of soft tissue, and can theoretically be applied to multiple skeletal sites using the critical-angle axial transmission ultrasound technique [37]. Madsen et al. [38] showed RA-related demineralization as quantified by three different QUS technologies, including the Ominsense device, and compared this with DXA.

The aim of this study was to compare multisite QUS to DXR for quantification of cortical bone loss depen-

dent on the severity of RA. Level of disease activity, influence of inflammation, and impact of soft tissue swelling were taken into account in the measurements of peripheral bone status as evaluated by DXR and multisite QUS.

Patients and Methods

Patients

This cross-sectional and comparative study enrolled 53 patients (39 female, 14 male). All patients underwent measurements of QUS (Sunlight multisite Omnisense 7000) with estimation of SOS (QUS-SOS) at the distal radius and at the phalanx of the third digit, as well as measurements of DXR-BMD and the metacarpal index (DXR-MCI) using DXR technology. All measurements were taken on the same day.

Mean age was 61.9 years, with a standard deviation (SD) of 10.4 years and a range of 20–83 years; all patients fulfilled the American College of Rheumatology 1987 revised classification criteria for RA [39]. No preselection regarding severity of RA was performed. Disease duration varied from 6 months to 44 years. Twenty patients were treated with methotrexate and 22 with a combination consisted of disease-modifying antirheumatic drugs and also nonsteroidal anti-inflammatory drugs. No patient had been on long-term prednisolone therapy. The remaining 11 patients had received neither disease-modifying antirheumatic drugs nor immune-modulating drugs. Subjects with abnormal renal function (serum creatinine > 130 μmol/L), on hormone replacement therapy/biphosphonates, or having other conditions known to affect bone metabolism (leukemia, Paget's disease, hyperparathyroidism) were excluded.

Classification of disease activity was based on the disease activity score, which has been revised to include a simplified, ungraded 28–joint count for tenderness (tender joint count, TJC) and for swelling (swollen joint count, SJC) called the DAS 28 [40, 41]. The DAS 28 is calculated as follows:

$$DAS\ 28 = (0.56 * TJC^{1/2}) + (0.28 * SJC^{1/2}) +$$
$$(0.7 * \ln[ESR]) + (0.014 * GH)$$

GH designates general health, as assessed by the patient using a 100 mm visual-analog scale ("How do you feel concerning your arthritis?": 0, very well; 100, extremely bad);

Ln[ESR] is the natural logarithm of the erythrocyte sedimentation rate (ESR in mm/1st hour; determined by the Westergreen method). DAS 28, a very sensitive parameter, is able to estimate level of disease activity in RA [40–42], differentiating between patients with minor disease activity (DAS ≤ 5.1) and those with an aggressive course of RA (DAS > 5.1).

DXR measurements were taken of the nondominant hand for each subject by digitally performed radiographs. In addition, digital radiographs of the dominant hand and of both feet were used to apply different scoring methods. Exclusion criteria were visible metallic material (i.e., splints and material after osteosynthesis) and signs of fracture (including presence of callus and bone deformities) in the entire right and left upper extremities.

All examinations were performed in accordance with the rules and regulations of the local human research and ethics committee. As a special note, the authors emphasize that all radiographs used for DXR calculation were performed as part of routine clinical care; no additional radiographs were obtained for study purposes.

For each patient, digital radiographs of both hands and both feet were independently scored by two radiologists using the Steinbroker stage and the Larsen score [43, 44] (Table 1). In cases of ambiguity, a third radiologist reviewed the radiographs; the individual sum of scoring points was then divided

Table 1. Definition of Larsen score and Steinbroker stage

Grade	Larsen score	Steinbroker stage
0	• Normal	—
1	• Periarticular demineralization • Soft tissue affection, initial reduction of joint space	• Periarticular demineralization
2	• Initial erosions and reduction of joint space	• Periarticular demineralization • Initial erosions
3	• Significant erosions and reduction of joint spaces	• Evident erosions • Reduction of joint spaces • Subluxation
4	• Partial ankylosis	• Ankylosis
5	• Ankylosis or mutilation	—

Fig. 1. Localization of ROI for DXR technique (yellow, metacarpal bones II-IV) and for QUS device (red, phalanx of the third digit).

by the evaluated joints, and the patients were subdivided into the different groups of grading.

DXR

The Pronosco X-Posure System™ (version 2.0; Pronosco/Sectra, Herlev, Denmark) was used to determine DXR-BMD and DXR-MCI based on radiogeometric analysis of metacarpal bones, requiring radiographs of the nondominant hand. All plain radiographs of the hand were acquired by a Polydoros SX_80 (Siemens, Munich, Germany) under the following standardized conditions: filter with 1.0 mm thickness related to aluminium 80, tube voltage 42 kV, exposure level 4 mAs, film focus distance 100 cm, Scopix Laser 2 B 400 (Agfa GmbH and Cie KG, Cologne, Germany).

Digital radiographs were subsequently printed and then scanned into the system by a high-resolution flatbed scanner (3,600 × 3,600 dpi, 12-bit resolution, 5.5 lp/mm); radiographs did not undergo special manipulation or edge enhancement before use for DXR analysis. The system itself checked the quality of the scanned images and interrupted the examination in case of inadequate quality. The computer algorithms automatically defined regions of interest (ROIs) around the narrowest bone parts of metacarpals II-IV (Fig. 1) and subsequently detected the outer and inner cortical edges of the included cortical bone parts.

The detection of the inner cortical edge by DXR is responsible for the precise calculation of the cortical thickness of the metacarpals and, consequently, the DXR-BMD [16, 18]. In the image analysis of DXR, the inner cortical edge is associated with the intensity maximum of the intensity profile across the bone of interest. For a bone with thick cortical tissue, the intensity maximum is located on a broader and less curved top than for a bone with a thin cortical shell. Thus, the position of the intensity maximum is more precisely defined on the narrow top of a thin bone than on the broader top of a thick bone. In each ROI, the cortical thickness and porosity were measured 118 times per centimeter, symmetrically around the center of the metacarpals. The analyzed images and their ROIs were displayed on the computer (Fig. 1). No manual manipulation of the ROI positioning is possible; thus, the DXR results could not be influenced by the operator.

The combined cortical thickness of a single metacarpal bone (MCP-CT) was calculated as the sum of the ulnar and radial cortical thickness (estimated in millimeters). An average value of the combined cortical thickness of the second, third, and forth metacarpal bones was calculated using the following formula:

$$(MCP - CT_2 + MCP - CT_3 + MCP - CT_4)/3$$
$$= MCP - CT_{mean}$$

Subsequently, the cortical volume per area (VPA) was calculated for each bone. DXR-BMD, based on the mean VPA, was computed with a correction for the estimated porosity, which was derived from the area percentage of local intensity minima found in the cortical part of the bone relative to the entire cortical area. DXR-BMD was estimated in grams per square centimeter. DXR-MCI obtains the mean cortical thickness normalized with the mean outer bone diameter. The data in this study are also shown with T and Z scoring, as recommended by Wuster et al. [45]. Only the T-score values for DXR-MCI are still not available. More details regarding this new method and the mathematical models used are given by Rosholm et al. [18].

QUS

Ultrasonic data acquisition was performed using the Omnisense 7000 device, which functions by accessing the bone from only one site and can be applied to multiple skeletal sites. Measurements of SOS were carried out by the same trained operator at the distal third of the radius and at the phalanx of the third digit of the nondominant hand (Fig. 1). The point of

Table 2. Intra- and interobserver reproducibility of QUS parameters differentiated for disease activity of patients with RA and for BMI of healthy individuals ($n = 12$)

	QUS-SOS (phalanx)			QUS-SOS (radius)		
	Mean (m/s)	SD (m/s)	CV (%)	Mean (m/s)	SD (m/s)	CV (%)
Intraobserver reproducibility						
Norm-weight (BMI ≤ 30)	3,721.34	17.86	0.48	3,954.12	17.40	0.44
Overweight (BMI > 30)	3,484.78	56.11	1.61	3,689.67	38.37	1.04
Low disease activity (DAS ≤ 5.1)	3,671.44	29.74	0.81	3,937.43	23.23	0.59
Advanced disease activity (DAS > 5.1)	3,484.27	69.00	1.98	3,858.94	44.76	1.16
Interobserver reproducibility						
Norm-weight (BMI ≤ 30)	3,743.55	32.94	0.88	3,971.65	27.40	0.69
Overweight (BMI > 30)	3,622.32	84.40	2.33	3,859.65	52.11	1.35
Low disease activity (DAS ≤ 5.1)	3,637.11	35.28	0.97	3,947.83	28.03	0.71
Advanced disease activity (DAS > 5.1)	3,543.88	99.58	2.81	3,877.92	55.45	1.43

probe placement for the measurement of the distal radius was defined as the point halfway between the edge of the olecranon to the tip of the distal phalanx of the third digit of the non-dominant hand. Ultrasound gel was applied to the skin at the sites selected for measurement, to facilitate acoustic coupling. The transducer was placed on the marked site of measurement and rotated by the operator without lifting it from the skin.

The Omnisense technology measures bone SOS by executing a complex measurement sequence based on Sunlight's proprietary and critical-angle axial transmission ultrasound technology. The Sunlight device uses a hand-held probe, which measures SOS at different sites. The probe contains a number of transducers, some acting as transmitters and the others as receivers, and is positioned on one site of the bone. Pulsed waves at a central frequency of 1.25 MHz are generated. The waves traverse the soft tissue on their way in and out of the bone and enter the bone at the so-called critical angle, which is a function of the SOS within the two media, soft tissue and bone. A part of the ultrasonic waves travels along the long axis of the bone within the outer 2–6 mm of the cortical bone matrix. The travel speed reflects the nature of the bone's properties. That part of the wave which is detected by the receiving transducers represents the fastest possible wave through the bone. Thus, it reflects the strongest cortical components of the measured bone partition. The received ultrasonic signal is digitized and analyzed by special software, and the SOS is evaluated by the system. SOS measurements must be performed repeatedly. When the SOS score was reproducible three times in a row at the premarked location, this measurement was used, converted to an age- and gender-matched Z score, and the T-score was estimated, adapted for adults [46]. Quality-control measurements of the Omnisense device (Sunlight Medical, Tel Aviv, Israel) were checked daily using a Perspex phantom provided by the manufacturer.

Short-Term Precision

Our measured precision for both techniques was comparable to reports in the literature by other research groups [15, 16, 38]. In this study, the following data of reproducibility for DXR measurements is expressed as the root mean square coefficient of variation. The short-term precision accounted for DXR-MCI 0.23% (healthy) vs. 0.21% (RA) and for DXR-BMD 0.17% (healthy) vs. 0.19% (RA). A differentiation of the reproducibility data based on body mass index (BMI) and disease activity is not required for the DXR because this method is not influenced by soft tissue alterations.

In contrast to many protocols, this *in vivo* study evaluated both inter- and intraobserver reproducibility of the multisite QUS-SOS device (phalanx and radius) and differentiated between patients with minor and those with advanced disease activity as well as healthy individuals with normal or elevated

BMI. Healthy individuals represented the following groups of BMI: norm-weight (BMI ≤ 30) and overweight (BMI > 30) controls. Additionally, reproducibility data were calculated for patients with RA differentiated into those with advanced disease activity (DAS 28 > 5.1) or low disease activity (DAS 28 ≤ 5.1).

Interobserver reproducibility of QUS-SOS was evaluated by three trained observers with 10 repeated measurements at the distal radius and third phalanx of three patients with RA versus healthy controls for each subgroup on the same day.

To verify intraobserver reproducibility, a single observer performed 10 repeated QUS-SOS estimates with all 12 individuals.

The values for QUS-SOS (phalanx) and, to a lesser extent, for QUS-SOS (radius) showed a significant difference ($P < 0.05$) between RA patients with low and those with accentuated disease activity and between healthy subjects with low and high BMI (Table 2); additionally, a significant difference ($P < 0.01$) was verified between healthy norm-weight subjects and RA patients with advanced disease activity.

Data Analysis

Results are expressed as means ± SD. Comparisons of parameters between QUS and DXR data were performed based on linear regression analysis ($P < 0.05$). The significance of severity-dependent bone loss was calculated with the Mann Whitney U-test. Statistical analysis was performed using SPSS version 10.13 (SPSS, Chicago, IL, USA) for Windows.

Results

Correlation of DXR and QUS

For all patients, DXR-BMD and DXR-MCI of the metacarpals were significantly correlated to multisite QUS-SOS of the radius and phalanx. Close associations, which compared both techniques, were observed between DXR parameters and QUS-SOS of the radius (for DXR-BMD R = 0.49, $P < 0.05$; for DXR-MCI R = 0.40, $P < 0.05$). Coefficients of correlation between DXR parameters to QUS-SOS (radius) were higher compared to QUS-SOS (phalanx) (for DXR-BMD 0.36 and for DXR-MCI 0.35, $P < 0.05$). Close correlations were found for DXR-MCI versus DXR-BMD with R = 0.79 ($P < 0.01$) and for QUS-SOS (radius) versus QUS-SOS (phalanx) with R = 0.62 ($P < 0.01$).

Table 3. Associations between DXR and QUS-SOS parameters differentiated for disease activity (DAS 28 ≤ or > 5.1) (n = 53)

	DXR-BMD	DXR-MCI	QUS-SOS (radius)
DAS ≤ 5.1 (n = 40)			
DXR-MCI	R = 0.83 (P < 0.01)		
QUS-SOS (radius)	R = 0.37 (P < 0.05)	R = 0.46 (P < 0.05)	
QUS-SOS (phalanx)	R = 0.66 (P < 0.01)	R = 0.52 (P < 0.05)	R = 0.74 (P < 0.01)
DAS > 5.1 (n = 13)			
DXR-MCI	R = 0.78 (P < 0.01)		
QUS-SOS (radius)	R = 0.71 (P < 0.01)	R = 0.84 (P < 0.01)	
QUS-SOS (phalanx)	R = 0.24 (P = n.s.)	R = 0.09 (P = n.s.)	R = 0.13 (P = n.s.)

n.s., not significant

Table 4. Comparison between patients with minor and accentuated disease activity (n = 53)

	DAS < 3.2 inactivity (n = 21)	3.2 < DAS < 5.1 low activity (n = 19)	DAS > 5.1 accelerated activity (n = 13)	Reduction from DAS < 3.2 to DAS > 5.1 (%)
DXR-BMD (gm/cm) (SD)	0.56 (0.09)	0.48 (0.08)	0.47 (0.05)	−16.1 (P < 0.001)
T score (SD)	−1.3 (1.6)	−2.1 (1.3)	−2.5 (1.0)	
Z score (SD)	−0.3 (1.3)	−1.3 (1.5)	−1.4 (0.6)	
DXR-MCI (SD)	0.39 (0.08)	0.37 (0.06)	0.32 (0.07)	−17.9 (P < 0.001)
Z score (SD)	−0.6 (0.8)	−0.8 (1.1)	−1.4 (0.9)	
QUS-SOS (radius) (m/s) (SD)	3,992.6 (186.6)	3,824.3 (179.8)	3,785.0 (139.7)	−5.2 (P < 0.05)
T score (SD)	−1.6 (2.0)	−2.0 (1.8)	−2.5 (1.8)	
Z score (SD)	−1.1 (1.7)	−1.2 (1.5)	−1.4 (1.4)	
QUS-SOS (phalanx) (m/s) (SD)	3,708.0 (208.6)	3,649.7 (166.0)	3,619.0 (204.5)	−2.4 (n.s.)
T score (SD)	−2.2 (1.5)	−3.0 (1.2)	−3.4 (1.5)	
Z score (SD)	−1.6 (1.3)	−2.1 (0.9)	−2.2 (1.5)	

n.s., not significant
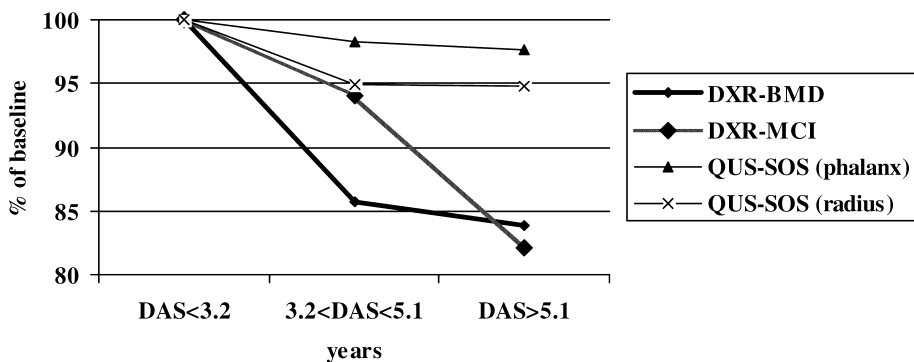
Fig. 2. Reduction of DXR and QUS-SOS parameters dependent on DAS 28.

Comparison of DXR and QUS Differentiated for Disease Activity

For the group with minor disease activity (DAS 28 ≤ 5.1), QUS-SOS (phalanx) was significantly associated to DXR-BMD (R = 0.66, P < 0.01) and DXR-MCI (R = 0.52, P < 0.05). Lower correlation coefficients were revealed between QUS-SOS (radius) and DXR parameters (DXR-BMD R = 0.37, P < 0.05; DXR-MCI R = 0.46, P < 0.05). In the case of high disease activity (DAS 28 > 5.1), QUS-SOS (radius) showed a close correlation to DXR-BMD (R = 0.71, P < 0.01)

and DXR-MCI (R = 0.84, P < 0.01), which surpassed the correlation coefficients compared to patients with minor activity of RA. For QUS-SOS (phalanx), no significant correlations to the DXR parameters were observed. Finally, DXR parameters revealed a close association among themselves independent of disease activity, whereas a significant correlation between the QUS parameters was verified only in patients with minor disease activity (R = 0.74, P < 0.01) (Table 3).

QUS-SOS and particularly the DXR parameters clearly revealed a decline in patients with increased disease activity compared to individuals with minor

Table 5. Reduction of DXR and QUS parameters from grade 1 to 5 (Larsen score) dependent on severity of RA ($n = 53$)

	Grade 1 mean (SD, $n = 10$)	Grade 2 mean (SD, $n = 16$)	Grade 3 mean (SD, $n = 10$)	Grade 4 mean (SD, $n = 9$)	Grade 5 mean (SD, $n = 8$)	Relative decrease from grade 1 to grade 5 (%)
DXR-BMD (g/cm^2)	0.58 (0.08)	0.49 (0.08)	0.46 (0.06)	0.44 (0.04)	0.43 (0.09)	−25.9 ($P < 0.01$)
T score	−0.1 (1.9)	−2.2 (1.4)	−2.5 (1.2)	−3.2 (0.9)	−3.4 (0.7)	
Z score	−0.6 (1.3)	−1.4 (1.2)	−1.8 (0.5)	−2.0 (1.9)	−2.2 (1.5)	
DXR-MCI	0.44 (0.06)	0.34 (0.07)	0.33 (0.07)	0.28 (0.02)	0.27 (0.05)	−38.6 ($P < 0.01$)
Z score	−0.2 (0.7)	−1.0 (0.9)	−1.4 (0.9)	−2.0 (0.7)	−2.1 (0.5)	
QUS-SOS (radius) (m/s)	3,994.4 (153.6)	3,915.8 (153.2)	3,969.7 (182.5)	3,825.5 (189.6)	3,890.3 (215.3)	−2.6 (P = n.s.)
T score	−2.1 (0.8)	−2.3 (1.7)	−1.5 (1.6)	−3.5 (1.7)	−2.5 (2.0)	
Z score	−1.2 (0.9)	−1.3 (1.3)	−0.3 (1.7)	−1.7 (1.1)	−1.1 (1.3)	
QUS-SOS (phalanx) (m/s)	3,566.8 (187.0)	3,470.4 (250.5)	3,639.1 (174.1)	3,481.3 (208.1)	3,428.7 (208.7)	−3.9 (P = n.s.)
T score	−3.1 (1.1)	−3.5 (1.6)	−2.3 (1.0)	−3.7 (1.2)	−3.3 (0.4)	
Z score	−2.2 (0.3)	−2.3 (1.2)	−1.0 (1.2)	−2.2 (1.4)	−2.3 (0.9)	

n.s., not significant

Table 6. Reduction of DXR and QUS parameters from stage 1 to 4 (Steinbroker stage) dependent on severity of RA ($n = 53$)

	Stage 1 mean (SD, $n = 11$)	Stage 2 mean (SD, $n = 14$)	Stage 3 mean (SD, $n = 16$)	Stage 4 mean (SD, $n = 12$)	Relative decrease from stage 1 to stage 4 (%)
DXR-BMD (g/cm^2)	0.59 (0.08)	0.48 (0.07)	0.45 (0.06)	0.43 (0.09)	−27.1 ($P < 0.01$)
T score	−0.1 (1.9)	−2.2 (1.5)	−2.8 (1.1)	−3.2 (0.9)	
Z score	−0.7 (1.4)	−1.5 (1.4)	−1.8 (0.5)	−2.1 (1.9)	
DXR-MCI	0.45 (0.05)	0.35 (0.05)	0.31 (0.06)	0.28 (0.05)	−38.6 ($P < 0.01$)
Z score	−0.2 (0.7)	−1.0 (1.0)	−1.6 (0.9)	−2.1 (0.5)	
QUS-SOS (radius) (m/s)	3,996.6 (153.6)	3,911.2 (161.5)	3,924.9 (183.2)	3,890.3 (215.3)	−2.7 (P = n.s.)
T score	−3.1 (1.0)	−3.4 (1.7)	−2.9 (1.3)	−3.7 (0.4)	
Z score	−2.2 (0.3)	−2.3 (1.2)	−1.4 (1.3)	−2.3 (0.9)	
QUS-SOS (phalanx) (m/s)	3,570.0 (176.6)	3,461.9 (271.0)	3,587.0 (185.0)	3,428.7 (208.7)	−4.0 (P = n.s.)
T score	−2.0 (0.8)	−2.2 (1.7)	−2.2 (1.8)	−2.5 (1.0)	
Z score	−1.2 (0.9)	−1.4 (1.4)	−0.8 (1.6)	−1.1 (1.3)	

n.s., not significant

activity (up to −17.9% for DXR-MCI and −5.2% for QUS-SOS radius), which could be also confirmed by the T and Z scores of both methods (Table 4, Fig. 2).

Severity-Dependent Reduction of QUS and DXR Parameters

Larsen score. DXR-BMD showed a significant decline (−25.9%) from 0.58 g/cm^2 ± 0.08 (grade 1) to 0.43 g/cm^2 ± 0.09 (grade 5), and DXR-MCI also revealed a reduction (−38.6%) from 0.44 ± 0.06 (grade 1) to 0.27 ± 0.05 (grade 5). QUS-SOS (radius) decreased from 3,994.4 ± 153.6 m/s (grade 1) to 3,890.3 ± 215.3 m/s (grade 5), with a relative reduction of −2.6% (P = nonsignificant). Regarding QUS-SOS (phalanx), a reduction of −3.9% (P = nonsignificant) from 3,566.8 ± 187.0 m/s (grade 1) to 3,428.7 ± 208.7 m/s (grade 5) was observed (Table 5).

The T and Z scores of both methods also revealed severity-dependent cortical bone loss, pronounced for DXR-BMD with a T score of −3.4 in grade 5.

Steinbroker stage. For Steinbroker stage, DXR-BMD significantly decreased (−27.1%) from 0.59 g/cm^2 ± 0.08 (stage 1) to 0.43 g/cm^2 ± 0.09 (stage 4). In this context, the relative reduction of DXR-MCI was −38.6% (P < 0.01). QUS-SOS (radius) showed a decline of −2.7% (P = nonsignificant) from 3,996.6 ± 153.6 m/s (stage 1) to 3,890.3 ± 215.3 m/s (stage 4), whereas QUS-SOS (phalanx) showed a relative decrease of −4.0% (P = nonsignificant) (Table 6).

In addition, the T and Z scores of both techniques demonstrated continued cortical demineralization dependent on the severity of RA.

Discussion

Correlations of DXR and Multisite QUS

It is common knowledge that various measurement sites, various osteodensitometric techniques, and different devices of the same technique result in significant dif-

ferences in estimated BMD values [47]. Based on this experience, our data revealed a quite close association between the QUS and DXR parameters, which is most likely due to the fact that multisite QUS and DXR principally quantify disease-related alterations of the cortical bone tissue.

This comparative study showed a closer association between QUS-SOS (radius) and DXR-BMD as well as DXR-MCI in comparison to QUS-SOS (phalanx). After adjustment for covariates, Madsen et al. [38] also reported a weak correlation (R = 0.38, P < 0.01) between multisite QUS-SOS (radius) and amplitude-dependent SOS (Ad-SOS) of the 2nd-5th phalanges evaluated by the DBM Sonic 1200. This study also surprisingly found no significant correlation between QUS-SOS (phalanx) and Ad-SOS (2nd-5th phalanges) and even between the QUS parameters of the Omnisense device itself [38]. In this respect, the clinically available QUS devices reveal a greater technological diversity than absorptiometric instruments based on different calibration methods, site of measurement, analysis software, and scanner design [11]; when considering these results from Madsen et al. [38], it may be important to note that the DBM Sonic device estimates SOS using the transmission technique and measures both cortical and trabecular bone matrix, whereas the multisite Omnisense technique measures only the cortical ultrasound speed along the bone surface based on the axial transmission (i.e., ultrasound reflection) technology.

Similar to the study from Madsen et al. [38], our data also show no significant association between QUS results measured at the phalanx or at the radius in patients with increased disease activity. Furthermore, QUS-SOS of the phalanx also showed no significant correlation to DXR-BMD and DXR-MCI in this group of patients.

Otherwise, close correlations between multisite QUS-SOS (radius) and DXR parameters were observed for patients with increased disease activity, whereas QUS-SOS (phalanx) significantly correlated with DXR-BMD and DXR-MCI for patients with less active RA.

To summarize, our data indicate that QUS-SOS measurements of the phalanx should not be recommended for patients with advanced disease activity of RA, whereas DXR functions independently of the effects of disease-related soft tissue alterations. Periarticular soft tissue edema, which particularly occurs during increased disease activity, seems to affect measurements of the multisite QUS-SOS at the phalanx and, to a lesser extent, at the radius (Table 2).

The limited applicability of the Omnisense device is in part due to its difficulty in precise correction for soft tissue influence as opposed to the DBM Sonic technique. The DBM Sonic device began each measurement with the determination of SOS through soft tissue at the interdigital region. The estimated value of the soft tissue

was taken into account to calculate a correction factor that is automatically applied by the system to the SOS results, when measuring the phalanx.

Steinschneider et al. [48] described the effect of soft tissue in healthy individuals for evaluation of bone status, as estimated by DXA and by the Omnisense device, using BMI. In the overweight group, QUS-SOS (phalanx) significantly correlated to DXA-BMD of the lumbar spine, but no close association could be observed for DXA-BMD of the femoral neck as well as for QUS-SOS of the radius and tibia. In contrast, healthy individuals with reduced BMI revealed significant associations between all QUS-SOS parameters (radius, tibia, and phalanx) and DXA-BMD of both the femoral neck and lumbar spine.

Barkmann et al. [37] showed a minor precision error, ranging 0.2−0.7%, for healthy women using the Omnisense device, while our short-term precision data showed marginally higher values for healthy norm-weighted subjects.

In contrast, RA patients with advanced disease activity showed a significantly increased precision error compared to healthy norm-weighted controls. The multisite Omnisense, which principally is a reflection technique, also revealed limitations in precision due to difficulties in repositioning of the device [25], which is confirmed by our experiences in clinical practice, particularly with RA patients.

Quantification of Disease Activity and Severity-Dependent Bone Loss with DXR and Multisite QUS

Generally, QUS data assessed by the DBM Sonic technique revealed significant peripheral bone loss in patients with prolonged RA [11, 26, 38, 49] and early RA [9, 26] in comparison with healthy controls or even osteopenic patients. To our knowledge, this is the first time that data have been presented on periarticular osteopenia of the hand in RA dependent on disease activity and severity of RA, as measured by DXR and compared to multisite QUS.

In patients with high disease activity, we found significant cortical bone loss, as measured by multisite QUS (radius) and DXR (Fig. 2), which reflects the observation that periarticular osteopenia is notably associated with the inflammation process itself [50].

Röben et al. [26] verified that patients with an advanced Larsen score (i.e., evidence of erosions) show accentuated cortical bone loss as estimated by Ad-SOS on the metaphysis of the phalanx. Only a slight decrease of cortical bone dependent on severity was estimated for the radius as well as the phalanx, as measured by multisite QUS-SOS in our study. It is not surprising that multisite QUS lacks accuracy in detecting cortical demineralization based on the level of disease activity and in particular severity-dependent cortical bone loss compared to DXR. This limitation could be caused by

the reduced short term precision of the multisite QUS device.

Previous studies [22, 23, 36, 51] have shown the potential of DXR-BMD as an indicator of joint damage. Additionally, Stewart et al. [24] reported that DXR is a reliable predictor for the erosive level of disease in RA individuals. The authors found that the reduction of DXR-BMD after 1 year was very specific (100%) and highly sensitive (63%) in detecting patients who developed an accelerated progress of RA with occurrence of erosions after a 4–year observation period. In addition, decreased DXR-BMD was independently associated with radiographic hand joint damage. In a comparative study between DXA and DXR, a relative decrease of DXR-BMD as well as DXR-MCI between the highest and lowest scores of the Steinbroker stage and Larsen score was documented, whereas the decrease of BMD using axial DXA measurements was not significant [22]. Another study reported a relatively significant reduction of trabecular BMD using peripheral quantitative computed tomography (pQCT), which varied from −10.3% to −16.9% (controlled by corticoid therapy), whereas no significant results could be verified for pQCT-BMD (cortical and total). A significant decrease was quantified for DXR-BMD up to −14.3% and for DXR-MCI up to −17.8% dependent on the severity of RA [52].

Agreeing with this data, DXR comparatively revealed a significant reduction of BMD and MCI dependent on the severity of RA in this study.

A limitation of DXR may be the measurement of only the cortical portion of BMD, which is less metabolically active compared to the trabecular bone tissue. However, cortical thinning of periarticular bone, supported by the inflammation process, is a typical phenomenon of bone destruction in RA [53, 54], which can be assumed because of very high bone turnover on the inner bone surface [55]. Recently, Dreher et al. [56] documented in a histopathological study that cortical-subchondral destruction is a common feature in early RA, whereas the origin of cortical destruction is not only the affected synovial tissue but also the inflammation-involved trabecular bone.

The influence of disease-related bony defects and erosions on the results of DXR can be minimized because DXR measures the diaphyseal part of the metacarpal bones. If the constancy of tube voltage and the assortment of appropriate digital imaging devices are standardized to achieve reliable results, the short-term precision of DXR is at a very low level [15], indicating that estimated demineralization is in fact disease-related and not based on the precision error of the densitometric method itself. Besides the operator-independent function of DXR, the high precision of DXR may also be explained by the procedure used to detect the inner cortical edges of a bone, particularly for patients with RA-related cortical thinning [16, 18].

Whether DXR and QUS techniques may serve as a useful approach for assessing fracture risk and disease progression before erosions occur remains to be clarified in prospective studies.

Conclusion

The development of digital imaging technology has advanced the precise measurement of several radiogeometric features. DXR is able to quantify disease-related BMD loss by thinning of the cortical bone dependent on RA severity. Possible applications and clinical importance of DXR might include a BMD calculation in routinely performed follow-up radiographs for monitoring the progression of RA and for confirming reparative changes after medical treatment. The operator-independent and computerized DXR technology could be an important diagnostic tool in RA, improving on the established scoring methods by offering quantitative data and, by early identification, promoting an optimized and timely therapeutic treatment for patients with an aggressive course of RA.

Multisite QUS and, to a significant extent, DXR are able to differentiate patients suffering minor disease activity and those with active RA as characterized by accelerated bone loss, indicated by the decreased values of DXR and QUS-SOS parameters.

In this study, the multisite QUS device was surpassed by DXR. In patients with accentuated disease activity, no significant association among the QUS parameters themselves and between QUS-SOS (phalanx) and the DXR parameters exists, and our reproducibility data regarding QUS-SOS reveal a limited short-term precision in RA patients with advanced disease activity. These data seem to indicate a significant influence of soft tissue swelling caused by active RA on QUS estimates at the phalanx and, to a lesser extent, at the radius as the measurement site. In patients with increased disease activity, QUS-SOS measurements at the radius should be preferred.

References

1. Brower AC (1990) Use of the radiograph to measure the course of rheumatoid arthritis. The gold standard versus fool's gold. Arthritis Rheum 33:316–324
2. Gough AK, Lilley J, Eyre S, Holder RL, Emery P (1994) Generalized bone loss in patients with early rheumatoid arthritis. Lancet 344:23–27

3. Hulsmans HMJ, van der Jacobs JWG, Heijde DMFM, van Albada-Kuipers GA, Schenk Y, Bijlsma JWJ (2000) The course of radiologic damage during the first six years of rheumatoid arthritis. Arthritis Rheum 43:1927−1940

4. Deodhar AA, Brabyn J, Jones BW, Davis MJ, Woolf AD (1995) Longitudinal study of hand bone densitometry in rheumatoid arthritis. Arthritis Rheum 37:1204−1210

5. Peel NF, Spittlehouse AJ, Bax DE, Eastell R (1994) Bone mineral density of the hand in rheumatoid arthritis. Arthritis Rheum 37:983−991

6. Dequeker J, Geusens P (1990) Osteoporosis and arthritis. Ann Rheum Dis 49:276−280

7. Dequeker J, Maenaut K, Verwilghen J, Westhovens R (1995) Osteoporosis in rheumatoid arthritis. Clin Exp Rheumatol 13:21−26

8. Sambrook PN (2000) The skeleton in rheumatoid arthritis: common mechanism for bone erosion and osteoporosis? J Rheumatol 27:2541−2542

9. Alenfeld FE, Diessel E, Brezger M, Sieper J, Felsenberg D, Braun J (2000) Detailed analyses of periarticular osteoporosis in rheumatoid arthritis. Osteoporos Int 11: 400−407

10. Devlin J, Lilley J, Gough A, Huissoon A, Holder R, Reece R, Perkins P, Emery P (1996) Clinical association of dual energy X-ray absorptiometry measurement of hand bone mass in rheumatoid arthritis. Br J Rheumatol 35: 1256−1262

11. Njeh CF, Boivin CM, Gough A, Hans D, Srivastav SK, Bulmer N, Delvin J, Emery P (1999) Evaluation of finger ultrasound in the assessment of bone status with application of rheumatoid arthritis. Osteoporos Int 9:82−90

12. Sambrook PN, Ansell BM, Foster S, Gumpel JM, Hesp R, Reeve J (1985) Bone turnover in early rheumatoid arthritis. 2. Longitudinal bone density studies. Ann Rheum Dis 44:580−584

13. Barnett E, Nordin B (1960) The radiological diagnosis of osteoporosis: a new approach. Clin Radiol 11:166−174

14. Black DM, Palermo L, Sorensen T, Jorgensen JT, Lewis C, Tylavsky F, Wallace R, Harris E, Cummings SR (2001) A normative reference database study for Pronosco X-posure System. J Clin Densitom 4:5−12

15. Böttcher J, Pfeil A, Rosholm A, Malich A, Petrovitch A, Heinrich B, Lehmann G, Mentzel HJ, Hein G, Linß W, Kaiser WA (2005) Influence of image-capturing parameters on digital X-ray radiogrammetry. J Clin Densitom 8:87−94

16. Jorgensen JT, Andersen PB, Rosholm A, Bjarnason NH (2000) Digital X-ray radiogrammetry: a new appendicular bone densitometric method with high precision. Clin Physiol 20:330−335

17. Malich A, Freesmeyer MG, Mentzel HJ, Sauner D, Böttcher J, Petrovitch A, Behrendt W, Kaiser WA (2003) Normative values of bone parameters of children and adolescents using digital computer-assisted radiogrammetry (DXR). J Clin Densitom 6:103−112

18. Rosholm A, Hylsdrup L, Baeksgaard L, Grunkin M, Thodberg HH (2001) Estimation of bone mineral density by digital X-ray radiogrammetry: theoretical background and clinical testing. Osteoporos Int 12:961−969

19. Shepherd JA, Meta M, Landau J, Sherrer YSR, Goddard DH, Ovalle MI, Rosholm A, Genant HK (2005) Metacarpal index and bone mineral density in healthy African-American women. Osteoporos Int Online first 10th June 2005

20. Bouxsein ML, Palermo L, Yeung C, Black DM (2002) Digital X-ray radiogrammetry predicts hip, wrist and vertebral fracture in elderly women: a prospective analysis from the study of osteoporotic fractures. Osteoporos Int 13:358−365

21. Hyldstrup L, Jorgensen JT, Sorensen TK, Baeksgaard L (2001) Response of cortical bone to antiresorptive treatment. Calcif Tissue Int 68:135−139

22. Böttcher J, Malich A, Pfeil A, Petrovitch A, Lehmann G, Heyne JP, Hein G, Kaiser WA (2004) Potential clinical relevance of digital radiogrammetry for quantification of periarticular bone demineralization in patients suffering from rheumatoid arthritis depending on severity and compared with DXA. Eur Radiol 14:631−637

23. Jensen T, Klarlund M, Hansen M, Jensen KE, Podenphant J, Hansen TM (2004) Bone loss in unclassified polyarthritis and early rheumatoid arthritis is better detected by digital radiogrammetry than dual X-ray absorptiometry: relationship with disease activity and radiographic outcome. Ann Rheum Dis 63:15−22

24. Stewart A, Mackenzie LM, Black AJ, Reid DM (2004) Predicting erosive disease in rheumatoid arthritis. A longitudinal study of changes in bone density using digital X-ray radiogrammetry: a pilot study. Rheumatology 43:1561−1564

25. Wuster C, Hadji P (2001) The use of quantitative ultrasound (QUS) in male osteoporosis. Calcif Tissue Int 69:225−228

26. Röben P, Barkmann R, Ullrich S, Gause A, Heller M, Gluer CC (2001) Assessment of phalangeal bone loss in patients with rheumatoid arthritis by quantitative ultrasound. Ann Rheum Dis 60:670−677

27. Njeh CF, Boivin CM, Langton CM (1997) The role of ultrasound in the assessment of osteoporosis: a review. Osteoporos Int 7:7−22

28. Antich P (1993) Ultrasound study of bone in vitro. Calcif Tissue Int 53:157−161

29. Brandenburger G (1993) Clinical determination of bone quality: is ultrasound an answer? Calcif Tissue Int 53:151−156

30. Duquette J, Honeyman T, Hoffman A, Ahmadi S, Baran D (1997) Effect of bovine bone constituents on broadband ultrasound attenuation measurements. Bone 21:289−294

31. Gluer CC, WU CY, Jergas M, Goldstein SA, Genant HK (1994) Three quantitative ultrasound parameters reflect bone structure. Calcif Tissue Int 55:46−52

32. Turner CH, Eich M (1991) Ultrasonic velocity as a predictor of strength in bovine cancellous bone. Calcif Tissue Int 49:116−119

33. Bauer DC, Gluer CC, Cauley JA, Vogt TM, Ensrud KE, Genant HK, Black DM (1997) Broadband ultrasound attenuation predicts fractures strongly and independently of densitometry in older women. A prospective study. Study of Osteoporotic Fractures Research Group. Arch Intern Med 157:629−634

34. Daens S, Peretz A, de Maertelaer V, Moris M, Bergmann P (1999) Efficiency of quantitative ultrasound measurements as compared with dual-energy X-ray absorptiometry in the assessment of corticoid-induced bone impairment. Osteoporos Int 10:278−283

35. Hans D, Dargent-Molina P, Schott AM, Sebert JL, Cormier C, Kotzki PO, Delmas PD, Pouilles JM, Breart G, Meunier PJ (1996) Ultrasonographic heel measurements to predict hip fractures in elderly women: the EPIDOS prospective study. Lancet 348:511−514

36. Haugeberg G, Orstavik RE, Uhlig T, Falch JA, Halse JI, Kvien TK (2003) Comparison of ultrasound and X-ray absorptiometry bone measurements in a case control study of female rheumatoid arthritis patients and randomly subjects in the population. Osteoporos Int 14: 312−319

37. Barkmann R, Kantrovitch E, Singal C, Hans D, Genant HK, Heller M, Gluer CC (2000) A new method for quantitative ultrasound measurements at multiple skeletal sites - first results of precision and fracture discrimination. J Clin Densitom 3:1−7

38. Madsen OR, Suetta C, Egsmose C, Lorentzen JS, Sorensen OH (2004) Bone status in rheumatoid arthritis assessed at peripheral sites by three different quantitative ultrasound devices. Clin Rheumatol 23:324−329

39. Arnett FC, Edworthy SM, Bloch DA, McShane DJ, Fies FJ, Cooper NS (1988) The American Rheumatism Association 1987 revised criteria for the classification of rheumatoid arthritis. Arthritis Rheum 31:315−324

40. Hettenkofer HJ (2004) Rheumatologie: Diagnostik - klinik - therapic, 5th ed. Thieme, Berlin
41. Van Gestel AM, Haagsma CJ, van Riel PL (1998) Validation of rheumatoid arthritis improvement criteria that include simplified joint counts. Arthritis Rheum 41:1845−1850
42. Aletaha D, Nell VP, Stamm T, Uffmann M, Pflugbeil S, Machold K, Smolen JS (2005) Acute phase reactants add little to composite disease activity indices for rheumatoid arthritis: validation of a clinical activity score. Arthritis Res Ther 7:R796−R806
43. Larsen A, Dale K, Eek M (1977) Radiographic evaluation of rheumatoid arthritis and related conditions by standard reference films. Acta Radiol Diagn 18:481−491
44. Steinbroker O, Traeger CH, Batterman RC (1949) Therapeutic criteria in rheumatoid arthritis. JAMA 140:659−662
45. Wuster C, Wenzler M, Kappes J, Rehm C, Gühring T, Arnbjerg C (2000) Digital X-ray radiogrammetry as a clinical method for estimating bone mineral density − a German reference database. J Bone Miner Res 15: 298
46. Zadik Z, Price D, Diamond G (2003) Pediatric reference curves for multisite quantitative ultrasound and its modulators. Osteoporos Int 14:857−862
47. Heilmann P, Wuster C, Prolingheuer C, Gotz M, Ziegler R (1998) Measurement of forearm bone mineral density: comparison of five different instruments. Calcif Tissue Int 62:383−387
48. Steinschneider M, Hagag P, Rapoport MJ, Weiss M (2003) Discordant effect of body mass index on bone mineral density and speed of sound. BMC Musculoskelet Disord 4:15−21
49. Martin JC, Munro R, Campbell MK, Reid DM (1997) Effects of disease and corticosteroids on appendicular bone mass in postmenopausal women with rheumatoid arthritis: comparison with axial measurements. Br J Rheumatol 36:43−49
50. Van der Heide A, Remme CA, Hofman DM, Jacobs JWG, Bijlsma JWJ (1995) Prediction of progression of radiologic damage in newly diagnosed rheumatoid arthritis. Arthritis Rheum 38:1466−1474
51. Böttcher J, Pfeil A, Lehmann G, Malich A, Hansch A, Heinrich B, Petrovitch A, Mentzel HJ, Hein G, Kaiser WA (2004) Clinical trial for differentiation between corticoid-induced osteoporosis and periarticular demineralization via digital radiogrammetry in patients suffering from rheumatoid arthritis. Z Rheumatol 63:473−482
52. Böttcher J, Pfeil A, Heinrich B, Lehmann G, Petrovitch A, Hansch A, Heyne JP, Malich A, Hein G, Kaiser WA (2005) Digital radiogrammetry as a new osteodensitometric technique and diagnostic tool in rheumatoid arthritis. Rheumatol Int 25:457−464
53. Kalla AA, Meyers OL, Parkyn ND, Kotze TJ (1989) Osteoporosis screening − radiogrammetry revisited. Br J Rheumatol 28:511−517
54. Kalla AA, Meyers OL, Chalton D (1991) Increased metacarpal bone mass following 18 months of slow acting antirheumatic drugs for rheumatoid arthritis. Br J Rheumatol 30:91−100
55. Jergas M (2003) Conventional radiographs and basic quantitative methods. In: Grampp S (ed), Radiology of osteoporosis, Springer, Berlin, pp 62−64
56. Dreher R, Thabe H, Schill S, Schulz A (2003) Die Rheumatoide Arthritis aus osteologischer Sicht. Osteologie 11(suppl 1):52